High Performance Computation of the Hybrid MoM/FDTD Code for health hazardous effects due to Mobile Base Station Antenna

H. A. Elsadek[1] Senior IEEE, H.H.Abdullah[1], M. Eldesouki[1], H. E. Eldeeb[1] and N. Bagherzadeh[2], Senior IEEE
1 Electronics Research Institute, Eltahrir st., Giza, Egypt, 12622, helsadek@eri.sci.eg.
2 The Henry Samueli School of Engineering, Electrical Engineering and Computer Science Dept., University of California, Irvine, CA 92697-2625, nader@uci.edu.

***Abstract*—With the rapid increase in wireless applications, the radiation from antennas has severe health hazards on human body if appropriate precautions are not taken into considerations. There is a need for measuring or calculating the specific absorption rate, SAR, inside the human body due to the illumination of the human body with the waves impinging from antennas' base stations. We propose instead of measuring the electromagnetic power, a simulation package that can replace these measurements. The simulation is cost effective method that doesn't need measuring equipment or specialists. The moment method is one of the most efficient numerical techniques that can get accurate results with minimum time consuming when dealing with antenna analysis. But it may be difficult and time consuming to simulate scattering inside an inhomogeneous dielectric material such as human body. The scattered field from the antenna simulated using the Method of Moment is applied as an incident wave in the FDTD simulator that is more efficient in SAR calculation in human body. Due to the large proposed problem size, these numerical techniques are heavy in computation that necessitates parallel processing technique to get the results with reasonable time consuming. This proposed algorithm helps people who live near base stations especially in ancient places where streets are too narrow and buildings are too close to each other. Also it would be useful for workers in these systems maintenance and installation. Different HPC platforms are applied as 4 node cluster, 16 core server with MPI middleware. Also, the code is run on 64 cores Bright Beowulf cluster. The SAR calculation due to one of the base stations antennas is introduced for code verification. Results comparison and verification are investigated.**

***Index Terms*—Method of Moment (MoM), Finite Difference time domain (FDTD), High Performance Computation, Specific Absorption Rate (SAR), Electric Field Integral Equation (EFIE).**

I. INTRODUCTION

AS growing as wireless communication in today's life, worldwide standard safety limits are set to regulate the interaction with human body. Specific absorption rate (SAR) is the factor to calculate with the RF/Microwave frequencies. Needless to say that the radiated power from base station/poster is hundreds of times greater than that radiated from mobile handheld device. This requires paying attention to its health hazardous effect on human body especially for workers in such fields, installation, maintenance, etc. Also an awareness of safety levels and the tools of their calculations are needed for persons live near such stations especially in Egypt ancient historical areas where streets are very narrow. From this extent the idea of this paper is to build a scientific tool for calculating such health effects in an accurate and fast way available anywhere at any time.

The calculations of base stations radiation effects require complex computer modeling with bulky computational effort [1]. FDTD is the most famous intensive full wave method that is used in these analyses. This is due its discretization nature that allows defining different characteristics of each cell. This is of course suitable for human body modeling which has tens of tissue layers and fluids with different inhomogeneous electrical and magnetic characteristics [2].

The basic restrictions in FDTD method are that it requires computing power with large memory workstations and long computational time. Run times for realistic human body together with an antenna can take hours, weeks or even longer on a high aspects PC. The slow nature of the algorithm resulted from the nested for-loops in FDTD that are required to iterate over three spatial dimensions (x, y, z) and time [3]. The memory constraint for such large problems (in order of millions of cells) makes the calculation is impossible for even fast PCs [4].

From this extent, this work aims to reach fast or even real time reliable model that calculates the mutual interaction between the human body and the electromagnetic wave exposure from mobile base stations.

Joseph and Martens [5] have studied the SAR distribution due to kathrein 736863 GSM base station antenna. They use the FDTD method for simulation and comparing the results with the measured data. The human body is simulated using a rectangular box phantom model. The results are not similar to the results obtained from the anatomically based model. So a correction factor is applied. After using the correction factor, a safety distance is calculated based on the input power to the antenna. So, a more accurate model for the human body is required to give better results. However in that study, the simulation of both the base station antenna and the human body will be time and memory consuming and the antenna model will not be accurate due to the stair case modelling of the antenna surface. So, one of the best solutions to this problem is to use a hybrid techniques such as Moment method to simulate the antenna and the FDTD to calculate the SAR distribution within the human body.

In [6] a hybrid method is applied to simulate the SAR distribution induced in a numerical phantom in front of the base

station helical antenna. The helical antenna is simulated by the time domain method of Moments. The electric and magnetic field that is radiated from the antenna is converted into magnetic and electric current in a Huygens's box. The Huygens's box acts as a source of electromagnetic radiation in the FDTD code. Then the FDTD can be used to simulate the SAR distribution using the Huygens box excitation. The results are stable but the accuracy is not very good. So there is a need for more cell refinement. But this refinement will be in the expenses of memory and time. In [7], the NEC software (a Moment method commercial solver) is used to analyze the base station antenna and the results are used as an excitation to the FDTD that calculates the SAR within the human head model. They use the Bradford University human head model in their calculations. Although the head model is not sufficient to model the whole body interaction, the authors uses the human head model as a test piece for the method. They used the half wavelength dipole antenna as a representation for the base station.

From the above discussion, there are still more difficulties in the determination of the health hazards on human body due to the base station radiations. These difficulties are confined to the need for accurate model for the human body, optimum numerical techniques for the calculation, the resources that fulfil the calculations requirements, and the most important factor, the execution time.

To shorten the computational time, people acquire faster computers, lease time on supercomputers, to gain a parallel processing speed up. Other researchers such as Tinniswood et. al. [8] have applied parallel processing to the 3D-FDTD method using a MeikoCS-2MPP (Massively–parallel processors) computer and the KSR-1 "virtual shared computer". These computers are specially designed for parallel processing and have high speed data links between processors [9]. These solutions can be expensive and frequently impractical. As a result for such literature survey, an approach that increases the speed of the FDTD method and at the same time relatively inexpensive and practical is required. Parallel processing for 3D-FDTD could be built over LANs to produce extremely large arrays with millions of cells [10]. These network solutions have the advantages that the computers can be used for other purposes when not simulating the method. Cluster/Grid computing is an efficient platform for such heavy computation applications [11]. A cluster/Grid computing offers several important advantages. Some of these advantages are better price/performance ratios, scaling to very large number of nodes, flexibility of configuration and easily upgrading [12]. The cloud computing is another parallel environment that is utilized for more economic and faster computational platform

II. PROBLEM FORMULATION

The hybrid MoM/FDTD algorithm is based on integrating the method of moments and the FDTD method to solve complex problems such as the SAR distribution within the human body in the vicinity of mobile base stations.

As shown in Figure 1, the hybrid MoM/FDTD algorithm starts by defining the geometric model of both the antenna and the human body model at the same time. The meshing of the antenna is based on triangulation of the antenna geometry to suite the MoM algorithm while the human body is modeled using cubic cells to suite the FDTD algorithm.

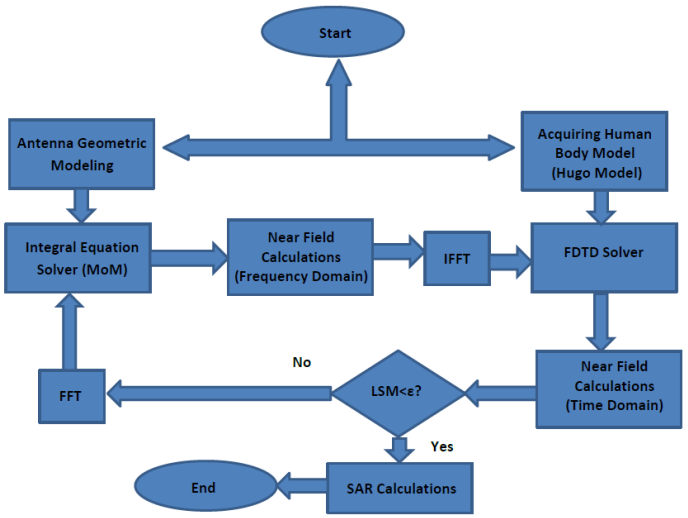


Fig. 1: The flow chart of the hybrid MoM/FDTD technique

Upon the preparation of the geometric modeling of both the antenna and the human body, the algorithm starts by solving the electric field integral equation (EFIE) using the MoM method according to the RWG basis function [14]. The result of the MoM solution is the current distribution over the whole edges of the triangles that constitute the base station antenna. By the knowledge of the current distribution on the antenna, one can calculate either the near or the far fields. The concept of the hybrid code is created from the use of the fields calculated using the MoM code as an incident field on the FDTD lattice. But the MoM code is a frequency domain solver while the FDTD is a time domain solver so, a fast Fourier transform is required to transform the fields calculated using the MoM to the time domain to suite the FDTD computational domain. The second step is to run the FDTD code in the presence of the human model with an incident fields from the antenna modeled by the MoM code. This is not an accurate computation since the interaction of the antenna and the human body is neglected. In order to take this interaction into account, the scattered field from the human body is used to excite the antenna again in the MoM code. Then the antenna analysis is repeated again taking into consideration the scattered field from the human body. Again the FDTD code is simulated with the updated scattered field from the antenna. This code running process needs to be repeated several times until the least mean square error between two successive FDTD runnings is below a certain value in such a way that the results could be considered accurate enough to be utilized. The final step is to calculate the SAR values using the available time domain field data within the different tissues of the human body.

1. Method of Moment MoM

The method of moments discussed in [14] is based on solving the electric field integral equation based on the boundary conditions at the surface of a conductor. The triangular meshing is used to model the geometric shape of the scattering structure (antenna in our case) because it makes the best fitting for complicating structures. The RWG basis used to discretize the current distribution over the structure. For brief, the algorithm [14] is summarized in the following steps

The algorithm transforms the EFIE into a linear system of equations in the form

$$[Z_{mn}][I_n] = [V_m] \quad (1)$$

Where

$$Z_{mn} = l_m l_n \left(\frac{j\omega\mu}{4\pi}\alpha_{mn} + \frac{1}{j\omega\pi\varepsilon}\beta_{mn}\right) \quad (2)$$

$$\alpha_{mn} = \alpha_{m^+n^+} + \alpha_{m^+n^-} + \alpha_{m^-n^+} + \alpha_{m^-n^-} \quad (3)$$

$$\beta_{mn} = \beta_{m^+n^+} + \beta_{m^+n^-} + \beta_{m^-n^+} + \beta_{m^-n^-} \quad (4)$$

$$\alpha_{m^\pm n^\pm} = \frac{1}{4A_{n^\pm}}\left(\int_{P_{n^\pm}} G_m^{c\pm}(\vec{f})\vec{\rho}_n^{\pm} d\acute{S}\right)\cdot\vec{\rho}_m^{\pm} \quad (5)$$

$$\beta_{m^\pm n^\pm} = \frac{(s_{m^\pm})(s_{n^\pm})}{4A_{n^\pm}}\left(\int_{P_{n^\pm}} G_m^{c\pm}(\vec{f}) d\acute{S}\right) \quad (6)$$

where

$$s_m = \begin{cases} +1, & m = m^+ \\ -1, & m = m^- \end{cases}, \text{ and } s_n = \begin{cases} +1, & n = n^+ \\ -1, & n = n^- \end{cases}$$

Note that, the plus or minus signs over m refers to the positive or negative observation patches respectively, while that over n refers to the source positive or negative patches respectively.

The $[V_m]$ is filled using the following equation

$$\langle \vec{E}^i, \vec{f}_m \rangle = \frac{l_m}{2}\left(\vec{E}^i(\vec{r}_m^{c+}).\vec{\rho}_m^{c+} + \vec{E}^i(\vec{r}_m^{c-}).\vec{\rho}_m^{c-}\right) \quad (7)$$

$\vec{E}^i(\vec{r}_m^{c+})$ is a pre-calculated function that represents the incident wave. It may be a feed point on an antenna or a plane wave incident on the body from a certain direction that is specified according to the specific problem structure. The code is run on a parallel cluster environment. The cluster is a group of computers in a network that work together. The parallel algorithm is based on our published paper [15].

2. FDTD Scattered Field Formulation

The incident field can be defined as the field that would be present in the absence of the scatterer, i.e. the field always propagates in free space (even when passing through the interaction object or scatterer material) while the scattered field is the resulting field due to the interaction of the incident field with the interacting object. The total field is the resultant field that would exist when adding both the incident and the scattered fields in the space domain. In order to demonstrate the idea of the scattered field formulation, the lossy dielectric structure is to be considered as in the following sections.

3. Application to Lossy Dielectric Structure

Starting with Maxwell's curl equations and writing them first for total field quantities

$$\mu\frac{\partial \overline{H}_{tot}}{\partial t} = -\nabla X\overline{E}_{tot} - \sigma^*\overline{H}_{tot} \quad (8)$$

$$\varepsilon\frac{\partial \overline{E}_{tot}}{\partial t} = \nabla X\overline{H}_{tot} - \sigma\overline{E}_{tot} \quad (9)$$

Note that the material parameters $\mu, \varepsilon, \rho',$ and σ are permitted to vary in an arbitrary manner throughout the space of interest for this total-field formulation. Regarding the incident field Maxwell's equations can be rewritten as

$$\mu_0\frac{\partial \overline{H}_{inc}}{\partial t} = -\nabla X\overline{E}_{inc} \quad (10)$$

$$\varepsilon_0\frac{\partial \overline{E}_{inc}}{\partial t} = \nabla X\overline{H}_{inc} \quad (11)$$

Note that the incident field propagating in vacuum is defined as having the electric parameters $\mu_0, \varepsilon_0, \sigma^* = 0,$ and $\sigma = 0.$

Now, under the assumption of the linearity of Maxwell's equations, one can divide the total field into the summation of the incident and the scattered fields yielding

$$\mu\frac{\partial \overline{H}_{scat}}{\partial t} + \sigma^*\overline{H}_{scat} = -\nabla X\overline{E}_{scat} - \sigma^*\overline{H}_{inc} - (\mu-\mu_0)\frac{\partial \overline{H}_{inc}}{\partial t} \quad (12)$$

$$\varepsilon\frac{\partial \overline{E}_{scat}}{\partial t} + \sigma\overline{E}_{scat} = \nabla X\overline{H}_{scat} - \sigma\overline{E}_{inc} - (\varepsilon-\varepsilon_0)\frac{\partial \overline{E}_{inc}}{\partial t} \quad (13)$$

Equations (12) and (13) can be realized numerically using ordinary Yee central differencing to implement the space derivatives of the curl or exponential time-stepping to implement the time derivatives.

4. The FDTD Near to Near Field Transformation

In the hybrid code, it is assumed that the MoM and FDTD domains are in the near field for both of them. So, the near to near field transformation is essential in this case.

The near and far fields are calculated in the FDTD using the Kirchhoff's surface integral representation (KSIR). In order to avoid the interpolation errors in the Yee scheme, the KSIR calculates the six field components based on the value of the same field component over a closed surface. The KSIR leads to highly accurate near fields that reduces absorbing boundary condition (ABC) errors [19].

Problem Formulation

The Kirchhoff's integral representation is a relationship between the field inside a closed volume V and the field with its derivatives on the surface of V:

$$\psi(r,t)=\frac{1}{4\pi}\oiint_{s}\hat{n}\cdot\left[\frac{\vec{\nabla}\psi(\acute{r},\acute{t})}{R}-\frac{\vec{R}}{R^3}\psi(\acute{r},\acute{t})-\frac{\vec{R}}{cR^2}\frac{\partial\psi(\acute{r},\acute{t})}{\partial\acute{t}}\right]_{ret}d\acute{s} \quad (14)$$

Where $\vec{R}=\vec{r}-\vec{\acute{r}}, R=|\vec{R}|, \hat{n}$ is the unit normal vector to the surface, c is the speed of light in free space, and ret indicates that the integrand is evaluated at the retarded time $\acute{t}=t-R/c$. ψ can be any of the six field components.

The derivation is done over only one plane where the derivation on the other planes is straight forward.

Without loss of generality, the surface in the xy-plane is chosen at k= k_0 , where k is the FDTD z index, and let $\psi = E_x$. We then employ a change of variable in the time domain; that is, instead of using retarded time, we express the calculated field as a function of the advanced time $t^*=t+R/c$. At time step n+1, the time and derivatives are approximated by a second-order accurate center difference formula

$$\left.\frac{\partial E_x^{n+1}}{\partial x}\right|_{k=k_0}=\frac{E_x^{n+1}(\acute{\imath},\acute{\jmath},\acute{k}_0+1)-E_x^{n+1}(\acute{\imath},\acute{\jmath},\acute{k}_0-1)}{2\Delta z} \quad (15)$$

$$\left.\frac{\partial E_x^{n+1}}{\partial x}\right|_{k=k_0}=\frac{E_x^{n+2}(\acute{\imath},\acute{\jmath},\acute{k}_0)-E_x^{n}(\acute{\imath},\acute{\jmath},\acute{k}_0)}{2\Delta t} \quad (16)$$

$$E_x(r,t_n^*)=\text{flag}*\sum_{\acute{\imath},\acute{\jmath}}\left(A\frac{E_x^{n+1}(\acute{\imath},\acute{\jmath},\acute{k}_0+1)-E_x^{n+1}(\acute{\imath},\acute{\jmath},\acute{k}_0-1)}{2\Delta z}+B_z E_x^{n+1}(\acute{\imath},\acute{\jmath},\acute{k}_0)+C_z\frac{E_x^{n+2}(\acute{\imath},\acute{\jmath},\acute{k}_0)-E_x^{n}(\acute{\imath},\acute{\jmath},\acute{k}_0)}{2\Delta t}\right) \quad (17)$$

Where $A=\frac{1}{4\pi R}$, $B_z=\frac{-(z-\acute{z})}{4\pi R^3}, C_z=\frac{-(z-\acute{z})}{4\pi cR^2}$ and $R=\sqrt{(x-\acute{x})^2+(y-\acute{y})^2+(z-\acute{z})^2}$.

After manipulations, the E_x component due to scattering from a plane normal to the z axis could be written in the form

$$E_x(r,t_n^*)=F_{1xz}(n)+F_{2xz}(n+1)+F_{3xz}(n+2) \quad (18)$$

$$F_{1xz}(n)=\text{flag}*\sum_{\acute{\imath},\acute{\jmath}}\frac{-C_z}{2\Delta t}E_x^{n}(\acute{\imath},\acute{\jmath},\acute{k}_0)\Delta_{\acute{\imath},\acute{\jmath}} \quad (19)$$

The flag here may be positive or negative sign that indicates if the normal to the surface is in the direction of the spatial coordinates or in the reverse direction, respectively.

$$F_{2xz}(n+1)=\text{flag}\left(\sum_{\acute{\imath},\acute{\jmath}}\frac{A}{2\Delta z}\left(E_x^{n+1}(\acute{\imath},\acute{\jmath},\acute{k}_0+1)-E_x^{n+1}(\acute{\imath},\acute{\jmath},\acute{k}_0-1)\right)\Delta_{\acute{\imath},\acute{\jmath}}+\sum_{\acute{\imath},\acute{\jmath}}B_z E_x^{n+1}(\acute{\imath},\acute{\jmath},\acute{k}_0)\Delta_{\acute{\imath},\acute{\jmath}}\right) \quad (20)$$

$$F_{3xz}(n+2)=\text{flag}*\sum_{\acute{\imath},\acute{\jmath}}\frac{C_z}{2\Delta t}E_x^{n+2}(\acute{\imath},\acute{\jmath},\acute{k}_0)\Delta_{\acute{\imath},\acute{\jmath}} \quad (21)$$

Test Case

Suppose that a plane wave is incident on a lossy dielectric sphere of relative dielectric constant of 4 and conductivity of 0.005 S/m. The radius of the sphere is 0.48 m. The applied boundary condition algorithm is the CPML. The computational domain is discretized into 50 X 50 X 50 cells. The discretization steps are 1/17 m in x, y and z directions. The incident field is a plane wave with Gaussian pulse signal as shown in Fig. 2. The scattered field is computed within the FDTD computational domain using the conventional FDTD method and compared to the proposed technique of the near to near field transformation. As shown from the figure, very good agreement is observed.

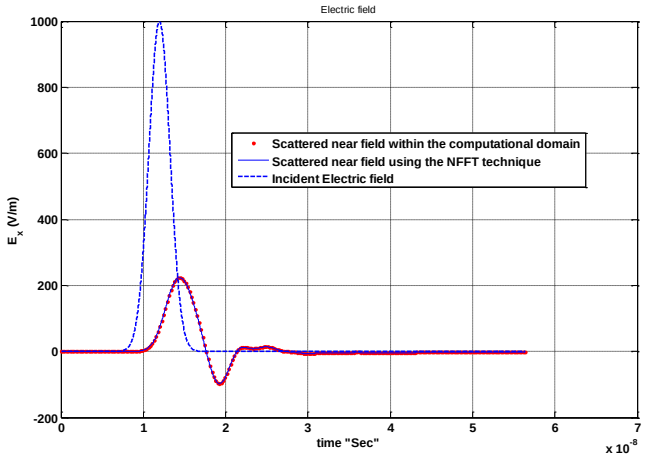


Fig. 2 Comparison between scattered field in the near field calculated using the NFTNF scheme component and the conventional FDTD

We are introducing the design and implementation of a 3D FDTD parallel algorithm that helps in solving the calculation of the SARs distribution inside the human body due to radiating antennas of wireless communications. The parallel algorithm is written using C language and MPI as a parallel environment middle ware. One of parallel processing strategies that are used in our algorithm is to divide the space among the available processors, such that each processor is responsible to calculate the electric and magnetic fields in its space. The domain decomposition can be in one, two or three dimensions; the 1D Domain decomposition technique was used in our application for simplifying data distribution and data dependency as the space is partitioned along the Z direction only as shown in Fig. (3).

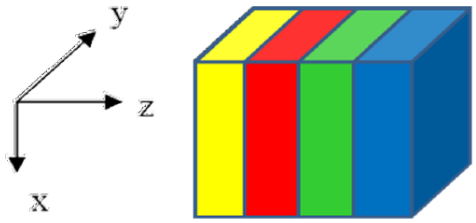


Fig. (3) 1D Domain Decomposition

The sub domain of each processor = (Nz/No. of processors) where, Nz is the size of the Z dimension, and the remainder of the devision is redistributed among the processors, for example if the domain size equal to [8][8][15] as shown in Fig. (4) then Nz=15.

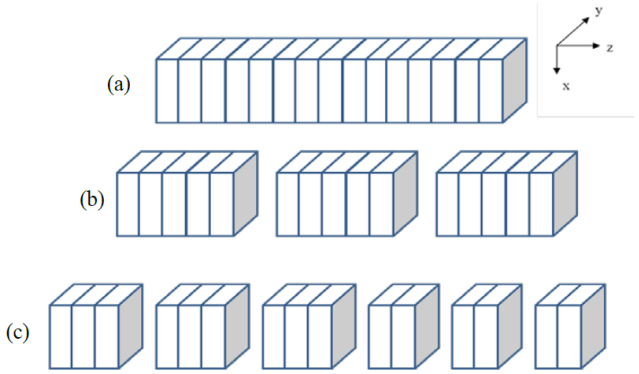


Fig. 4: Load Distribution on (a) 1, (b) 3 and (c) 6 Processors

The field at each time step is evaluated from the neighborhood fields in the previous time step. So the processors depend on each other for the boundaries values each one exchange the boundaries (electric and magnetic fields values) with its neighbors as shown in Fig. (5).

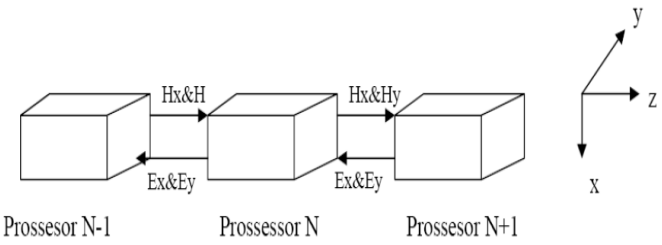


Fig. 5: Data Dependencies

As shown in Fig. (5), the tangential magnetic fields Hx and Hy are updated in the subdomain N, and then forwarded to the subdomain (N+1). They are then used as boundary conditions in the subdomain (N+1) to calculate the electric fields Ey and Ex on the subdomain (N+1) and then forwarded to the subdomain N. This procedure, which is repeated at each time step, requires that the electric field be exchanged between two subdomains following the updating of this field. Likewise the magnetic field is to be exchanged after its updating has been completed, and hence, the field exchange procedure is carried out twice in each time step. The parallel processing algorithm is based on our previously published paper [12].

III. RESULTS AND DISCUSSION

A simple dual-band dual-polarized aperture stacked patch antenna with double sided notch is presented [11]. This antenna is suitable for operation in telecommunication base stations. One of the bands covers the GSM band, while the other covers both DCS and UMTS bands. Two microstrip feed lines are placed on separate substrates on the opposite side of the ground plane. The polarization isolation is found out to be greater than 30dB in both bands. The antenna dimensions are about 290mm×220mm×21.8mm and its gain is about 11.8dBi and 7dBi for lower and upper bands, respectively. The antenna is simulated using the commercial package CST-microwave studio-2014 and our home made MOM code for code results verification. The step size in MOM is 2×2 mm2 while at the feed; the step size is 0.5×0.5 mm2. The meshing in CST is adaptive meshing with minimum mesh step of 0.21 mm and maximum mesh step of 1.54 mm. Figure 1 shows the antenna structure while Figure 6 shows the established geometric model for the antenna in MOM code. The SAR calculations are done by inserting the commercial Hugo model shown in Figure 8 within the parallel FDTD computational domain. The tissues that are contained have relative permittivity and conductivity, according to [16, 17]. The tissues frequency dispersive is normalized at the two center frequencies of the two base stations 'operating bands, 900 MHz and 1.8 GHz, respectively.

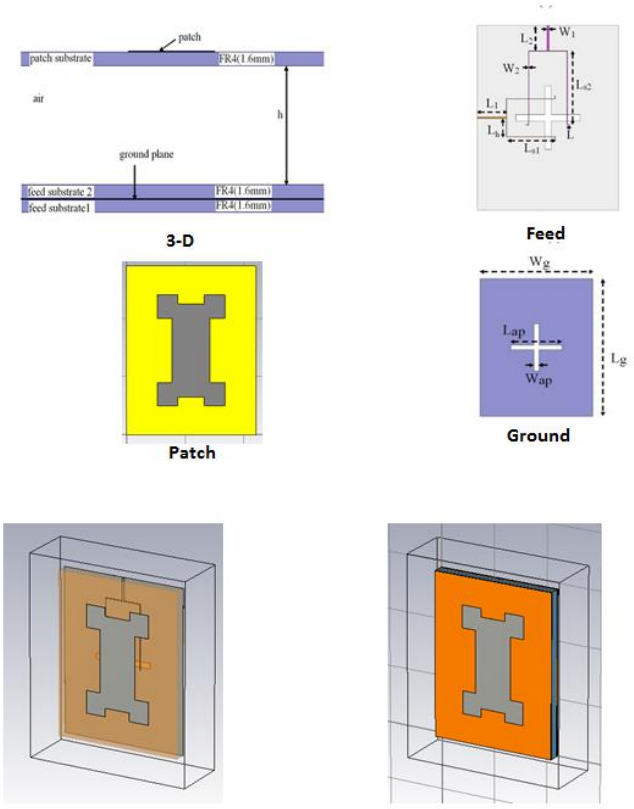


Fig. 6: structure of dual-band dual-polarized aperture stacked antenna

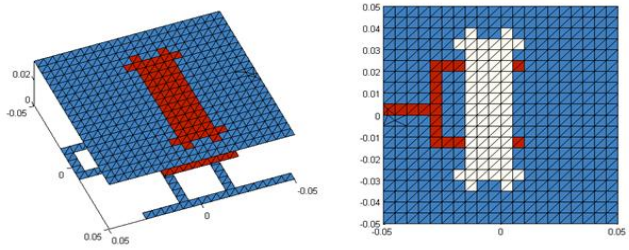


Fig. 7: The geometric model of one element of the base station antenna array

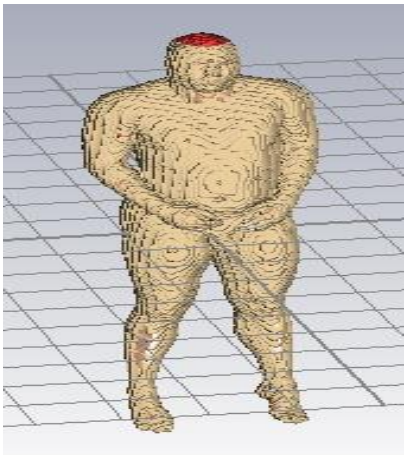


Fig. 8: The commercial Hugo Human model that utilized within the FDTD code

In this work a design for a multiband microstrip antenna for base station mobile applications is introduced using an FR4 commercial substrate with dielectric constant of 4.5, h = 1.5mm to operate at GSM 900, DCS 1800, and UMTS 2100. Our results are compared to the CST 2014 software. Fig. 7 shows the comparison of return loss of the antenna using MoM and CST where a good agreement is observed.

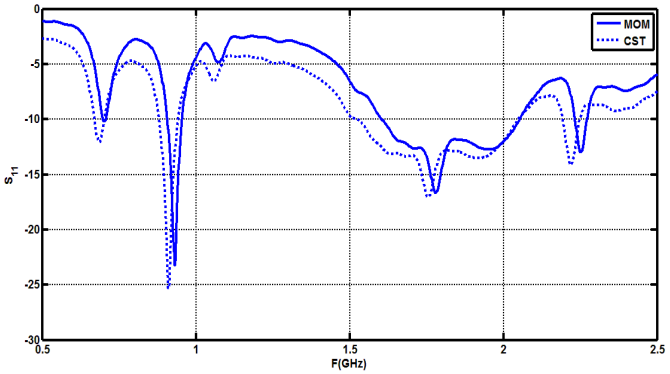


Fig. 9: Comparison of the return loss of the antenna element using CST and established MoM code for verification.**SAR distribution within the human body**

The SAR distribution within three different sensitive sections within the human body at 900 MHz is illustrated in the Figures (10, 11 and 12). The angle between the antenna and the human body is 450. It is noticed that the SAR within the Lungs sections is approximately double that within the eye section. The calculations are done by modeling the antenna in the MoM method as discussed in the previous section while the human body are modeled using the 170x126x366 unit cell Hugo model within the FDTD domain. The unit cell dimensions of the Hugo model is 6x6x6 mm3. The SAR value is calculated according to the following equation 22,

$$SAR = \frac{\sigma}{2\rho}|E_i|^2 \qquad (22)$$

Where E_i is the max value of the electric field strength in the tissue in V/m, σ is the conductivity of body tissue in S/m, and ρ is the density of body tissue in kg/m3.

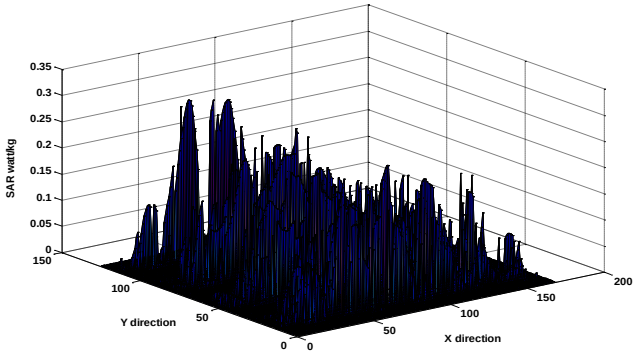


Fig.10: The SAR distribution within a section of the head passing through the eye at 900 MHz (Max. SAR value is 0.245 W/Kg)

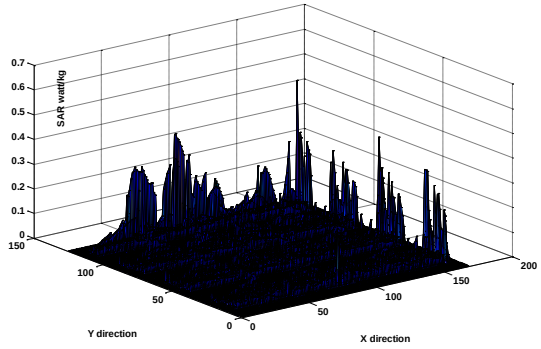


Fig.11: The SAR distribution within a section of the chest passing through the mid section of the lungs at 900 MHz (Max. SAR value is 0.5 W/Kg)

IV. PARALLEL COMPUTATION

The parallel hybrid code was written on standard C and MPI as a parallel environment middle ware tool, run on three different HPC-configurations with no change in the code configuration.

The parallel hybrid code firstly run on a 4 node cluster each with Intel(R) Pentium(R) Dual CPU Processor model, 2.40 GHz processor speed and the RAM memory is 4 GB.

The time reduced from 51.5 hrs when running on one processor to 28 hrs on 4 processors over the same environment as shown in Fig. 13.

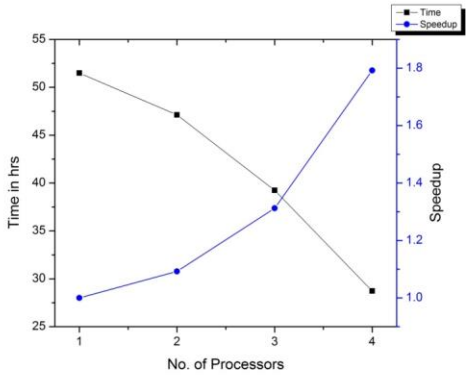


Fig. 13 Performance Analysis of the hybrid code over Cluster parallel environment

The parallel hybrid code run on a multicore server with Intel (R) Xeon (R) processor model, 2.93 GHz processor speed, two processors with 8 cores per processor. The RAM memory is 24 GB where the server is working under Scientific Linux / 64 Bit operating system. Fig. 14 illustrates the running time of the hybrid code over the aforementioned server and speedup gained at different number of Cores. The execution time at 16 cores is 3.6 times faster than the execution time at the serial code over the same environment.

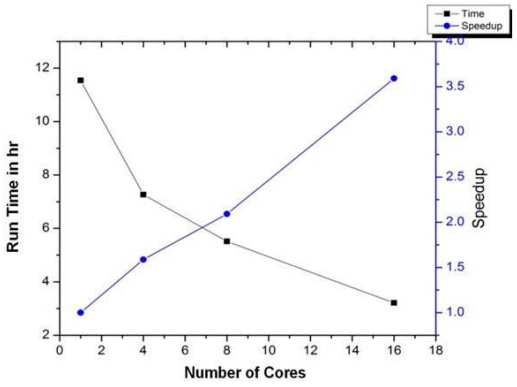


Fig.14: Performance Analysis of the hybrid code over the multicore server

The parallel hybrid code is then run on more powerful Bright Beowulf Cluster consists of a login, compile and job submission nodes, called the head node and six compute nodes, often referred to as worker nodes.

The head node has Intel (R) Xeon (R) processor model and speed 2.2 GHz, two processors each has physically 8 cores and RAM memory of 132 GB. While the worker nodes has Intel (R) Xeon (R) processor model and speed 2.7 GHz, two CPUs each has physically 8 cores and RAM memory of 132 GB.

Bright Beowulf cluster run Centos 6 operating system with MPICH is installed and configured as parallel programming environment. Fig. 15 shows the parallel hybrid code run time reduced from about 10 hrs. when running on one core to half an hour on 64 cores on the Bright Beowulf cluster, giving speed up to 19 times faster.

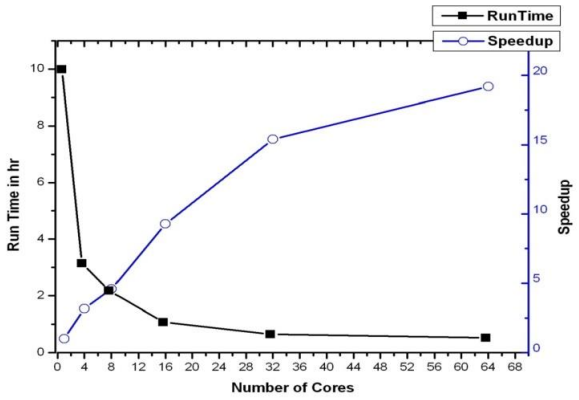


Fig 15: Performance Analysis of the hybrid code over the Bright Beowulf cluster

As Seen from the previous figures 13-15, the speed up gain increased with increasing the number of cores, The only limitation on speedup will be the domain size Nz, due to the load distribution and data dependencies in the sub domain of each core = Nz/No, where: No is the number of processors which must be greater than or equal 2 because of the data dependencies.

V. CONCLUSION

Parallel version of hybrid code compliance with major standards in the HPC field, such as standard C and MPI specifications, ensured compatibility of the parallel version with a broad range of HPC-configurations. As seen in the results the hybrid code computation time could be accelerated proportionally to the number of cores when parallel version is used. Such acceleration could be achieved with no changes in software configurations.

The only limitation on speedup will be the domain size Nz that the ratio Nz/No must be greater than or equal 2.

VI. ACKNOWLEDGMENT.

This work is funded by the Egypt Science and Technology Development Fund (STDF), contract No. 1968. Also The authors would like to acknowledge the STDF for the ERI grant number 5220 for HPC cloud Computing center of excellence.

I. REFERENCES

[1] Hesham Eldeep, Hala Elsadek, Haythem Abdallah, Maha Desouky, and Nader Bagherzadeh, "FDTD accelerator for calculating SAR distribution inside human head due to radiation from wireless devices," EMTS 2007 International URSI Commission B - Electromagnetic Theory Symposium • July 26-28, 2007 • Ottawa, ON, Canada.

[2] C. Gabriel, S. Gabriel and E. Corthout, "The dielectric properties of biological tissues: I. Literature survey," Phys. Med. Biol. Vol. 41, 1996, PP. 2231-2249.

[3] P. S. Excell and A. D. Limiswood, "A finite difference time domain program for parallel computers", Master thesis 1995, Queen Mary & Westfield college, July 1995.

[4] Amany Abd Elsamea, Hesham Eldeeb, Salwa Nassar "PC cluster as a plateform for parallel applications", Wseas Transactions on computers, pp.1220-1226, Vol. 3, Nov. 2004.

[5] Wout Joseph and Luc Martens, "Comparison of Safety Distances Based on the Electromagnetic Field and Based on the SAR for Occupational Exposure of a 900-MHz Base Station Antenna" IEEE Transactions on electromagnetic compatibility, vol. 47, Nov. 2005, Page(s):977 - 985.

[6] D. Lautru, J. Wiart, W. Tabbara', R. Mittra, "A MoMTD/FDTD hybrid method to calculate the SAR induced by a Base Station Antenna" Antennas and Propagation Society International Symposium, 2000. IEEE, 16-21 July 2000 Page(s):757 - 760 vol.2.

[7] Abd-Alhameed, R.A.; Excell, P.S.; Mangoud, M.A., "Computation of Specific Absorption Rate in the Human Body due to Base-Station Antennas Using a Hybrid Formulation", IEEE Transactions on Electromagnetic Compatibility,VOL. 47, May 2005, Page(s):374 – 381.

[8] A. D. Tinniswood, P. S. Excell, M. Hargreaves, S. Whittle, and D. Spicer, "Parallel computation of large-scale FDTD problems," Computation in Electromagnetic, Third International Conference on (Conf. publ. No. 420), 7-12, April 1996.

[9] A. D. Tinniswood, C. M. Furse, and O. P. Ghandhi, "Computations of SAR distribution for two anatomically based models of the human head using CAD files of commercial telephones and the parallelized FDTD code," Antennas and Propagation Society International Symposium, Digest, Vol. 2, 982{985, July 1997.

[10] J. Durbano, F. Ortiz and J. Humphery, "Hardware implementation of a three-dimensional finite-difference time-domain algorithm", IEEE antennas and wireless propagation letters, vol.2, 2003, PP: 54-57.

[11] Rao, S. M., D. R. Wilton, and A. W. Glisson, "Electromagnetic scattering by surfaces of arbitrary shape," IEEE Trans. Antennas Propagat., Vol. 30, No. 5, 409-418, 1982.

[12] Hussein, K. F. A., "Fast computational algorithm for EFIE applied to arbitrarily-shaped conducting surfaces," Progress in Electromagnetics Research, PIER 68, 339-357, 2007.

[13] H. H. Abdullah, F. M. EL-Hefnawi, and A. Z. Elsherbeni, "A FDTD Scattered Field Formulation for Dispersive Media," APS-2000, Salt Lake, PP. 248-251, July 2000.

[14] H. H. Abdullah, F. M. EL-Hefnawi, E. A. Hashish, and A. Z. Elsherbeni, Scattered Field FDTD Formulations for Debye Dispersive Media," URSI2001, International Conference on Electromagnetic in Advanced Applications ICEAA01, PP. 3-6, Sept. 10-14, Turin, Italy, 2001.

[15] H. H.Abdullah, F.M.EL-Hefnawi, E. A. Hashish, and A. Z. Elsherbeni, "Scattered Field FDTD Formulation for N-order Debye Dispersion Analysis," World Multi-conference on Systemic, Cybernetics and Informatics. ISAS SCI2001, PP. 122-125, July 22-25, Orlando, Florida, 2001.

[16] Omar M. Ramahi, " Near- and Far-Field Calculations in FDTD Simulations Using Kirchhoff Surface Integral Representation ," IEEE Transactions on Antennas and Propagation, vol. 45, May 1997, Page(s):753 - 759.